Experimental study on seismic behavior of steel strip reinforced CSPSWs in modular building structures

Xiao-Meng Dai [a], Yang Ding [a,b], Liang Zong [a,b,*], En-Feng Deng [a], Ni Lou [c], Yang Chen [d]

[a] *School of Civil Engineering, Tianjin University, Tianjin 300072, PRChina*
[b] *Key Laboratory of Coastal Civil Engineering Structure and Safety (Tianjin University), Ministry of Education, Tianjin 300072, China*
[c] *China National Engineering Research Center for Human Settlements, Beijing 100044, China*
[d] *CIMC Modular Building Systems Holding Co. Ltd., Jiangmen 529000, China*

ARTICLE INFO

ABSTRACT

Corrugated steel plate shear walls (CSPSWs) are widely used as exterior walls and efficient lateral load resisting systems in modular building structures (MBS). In practical construction, the CSPSWs are usually accommodated with door or window openings and reinforced with steel strips. The effect of the steel strip reinforcement needs to be evaluated. An experimental study was conducted to investigate the seismic behavior of steel strip reinforced CSPSWs in modular steel structures. Six full-scale specimens were constrained at corners and loaded with cyclic lateral load. The results showed that that failure mode of this lateral load resisting system for the modular building structures was the facture of the weld between the frame beams and columns. The steel strip reinforcement had little effect on the ultimate strength, but could improve the behavior of stiffness, ductility and energy dissipation.

1. Introduction

Corrugated steel plate shear walls (CSPSWs) have been widely constructed as efficient lateral load resisting system in the seismic hazard area. Due to exceptional strength, ductility and light weight, the corrugated steel plate shear walls are ideal for modular building structures (MBS). Corrugated steel plate shear wall usually consists of a rigidly connected frame and a corrugated thin steel plate infill. Compared with flat steel plate shear wall, the trapezoidal corrugations of the CSPSW provide out-of-plane stiffness, bringing higher lateral initial stiffness and avoiding the unpleasant buckling sound under very low load which impairs the living comfortability. Numerous studies have been conducted to investigate the lateral strength, stiffness, buckling behavior and energy dissipation capacity of corrugated steel shear wall systems and to propose prediction models. F. Emami etal. investigated the seismic behavior of horizontal and vertical CSPSWs under cyclic loads and the results showed that the direction of corrugations did not affect the seismic behavior significantly [1–3]. C. D. Zhou etal. [4] and J. Z. Tong [5] investigated the elastic buckling behavior of CSPSWs, giving predictions for the elastic buckling of the CSPSWs. M. Bahrebar etal. investigated the cyclic behavior of CSPSWs with numerical simulation and indicated the effectiveness of the web-plate thickness, corrugation angle, and opening size [6]. Effective non-linear analysis methods

was introduced to predict the seismic performance of the CSPSWs [7–9]. The seismic behavior of the CSPSWs in regular structures has been investigated.

For modular building structures, the CSPSWs are usually part of external walls and accommodated with door and window openings. The difference of the CSPSWs in regular and modular structures is the connection. In regular structures, CSPSWs are constrained on both upper and lower edges [10]. However, in modular steel structures, CSPSWs are constrained at corners as shown in Fig. 1. Besides, as the room modules of MBS are connected at corners, most of vertical load is transferred from upper column to lower column. The CSPSWs in modular steel structures mainly work as lateral load resisting system. The behavior of CSPSWs with and without openings has been investigated and the results show that the accommodated openings will significantly impair the performance of the CSPSWs [11]. As the openings are unavoidable in practical use, steel strips are attached on the CSPSWs as reinforcement. Steel strips are perpendicular to the corrugation and welded on each peak of the trapezoidal corrugations. These steel strips will strengthen the out-of-plane stiffness of the CSPSWs. Also these steel strips will improve the ductility and energy dissipation by constraining the deformation between peaks of corrugations. As the behavior of steel strip reinforced corrugated steel plate shear walls has not been investigated, effect of the steel strip reinforcement needs to be evaluated.

This paper presented an experimental study on seismic behavior of steel strip reinforced corrugated steel plated shear walls. Afull-scalequasi-static test program was reported. Six full-scale specimens

* Corresponding author.
E-mail address: zongliang@tju.edu.cn (L. Zong).

Vertical load on columns and shear walls

Lateral load

Constraint on upper and lower edge

(a) CSPSW in regular structures

Vertical load on columns

Lateral load

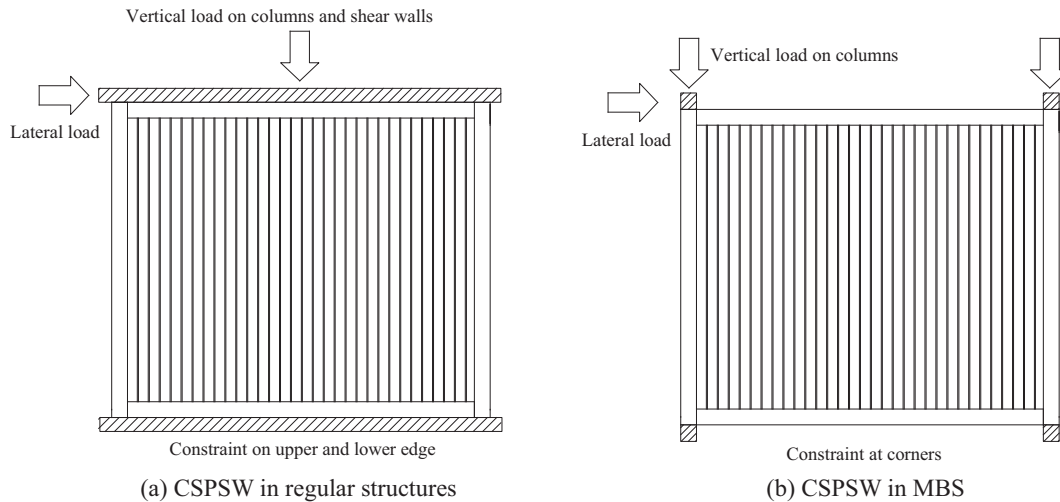Constraint at corners

(b) CSPSW in MBS

Fig. 1. Comparison of CSPSWs in regular structures and MBS.

were constrained at the lower corners to simulate the boundary conditions in modular steel structures. A cyclic lateral load was applied at the top corners. The results provided useful information on ultimate strength, initial stiffness, ductility and energy dissipation. The comparison was conducted that include variables of opening size and positions. Effect of the steel strip reinforcement was evaluated.

2. Experimental program

2.1. Specimen type

Totally, six specimens were designed and constructed to investigated and distinguish the seismic behavior of the corrugated steel plate shear walls with steel strip reinforcements. The shape of corrugations was shown in Fig. 2. All the specimens were constructed in full-scale, one-story and single-bay as represented in Fig. 3. The specimens were 3.0 m in height and 3.6 m in length. The design of the specimen was based on a CIMC construction project, which was a 19-storeycontainer-shaped modular steel construction. The structure plan was provided by CIMC, but the details were designed by authors. As there is no specialized standard for design of modular steel construction in China, this construction was designed on Chinese standard for steel construction [12]. Considering the corrugated steel plate shear walls was applied in modular building structures in which the sections of the girders and columns were limited, the surrounding frame section of the specimens was steel hollow square (SHS) section with dimensions of $150 \times 100 \times 6$ mm. The thickness of the corrugated steel plate was set as1.6 mm. Two pinned connecting cells were welded at the bottom of each specimen to simulate the connection between upper and lower modules in modular building structures.

All specimens were accommodated with respective openings. Among these specimens, the CSPSW-2, CSPSW-4 and CSPSW-6 were reinforced with steel strips while the rest were not. The steel strip was 100 mm in width, 4 mm in thickness and 360 mm in spacing. 5 rows of steel strips were set in each specimen. The trapezoidal corrugations were in vertical direction and the steel strips were horizontally welded

on the peaks of the corrugations with 360 mm-spacings. The specimens' details were shown in Table1.

2.2. Material properties

Mechanical properties of the steel plates and the steel profiles applied in the construction of the specimens were reported in Table2. The mechanical properties were determined by coupon test performed according to the GB/T 228.1–2010 [13]. The coupons were sampled from different parts of the specimens, i.e.,corrugated steel plates, steel strips, inner frames and outer frames. For each part of the specimens, four coupons were sampled and tested. Average values were taken from the each group of coupon test results. By a proper design, it ensured that the frame would not collapse before the infill corrugated steel plates reached the ultimate strength.

2.3. Test setup

The loading devices and facilities of the specimens were shown in Fig. 4. To simulate the boundary conditions in modular steel structures, the specimens were constrained at the lower corners. Two pinned connecting cells were welded at the bottom of each specimen. The specimens were connected to the fixed steel base with the pinned connecting cells. The steel base was anchored on the ground with six 60 mm-diameter bolts.

A loading hydraulic jack was connected to the top corner of the frame, applying a horizontal load to the specimen. The head of the hydraulic jack was pin-connected to the loading cell at the top right corner of the specimens. The rear of the loading hydraulic jack was fixed on a reaction wall. A dynamic force sensor was applied between the specimen and jack. An out-of-plane limiter was set on the top beam of the frame to prevent global instability by limiting the out-of plane displacement of the top beam. The limiter did not limit the lateral or vertical displacement so that the beam could move smoothly in the plane. No vertical load was applied to the specimens.

2.4. Loading program and measurements

To simulate earthquake load and investigate the seismic behavior of the CSPSWs, quasi-static cyclic load was applied with the loading hydraulic jack. The loading program consisted of pre-loading and normal loading program. During the pre-loading program, a cyclic load was applied and held at the load of 10% of predicted ultimate load for two minutes. The purpose of the pre-loading program was to make sure the specimen and the loading devices close fit. The data of pre-loading
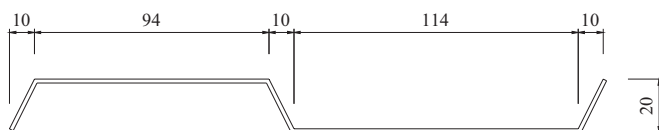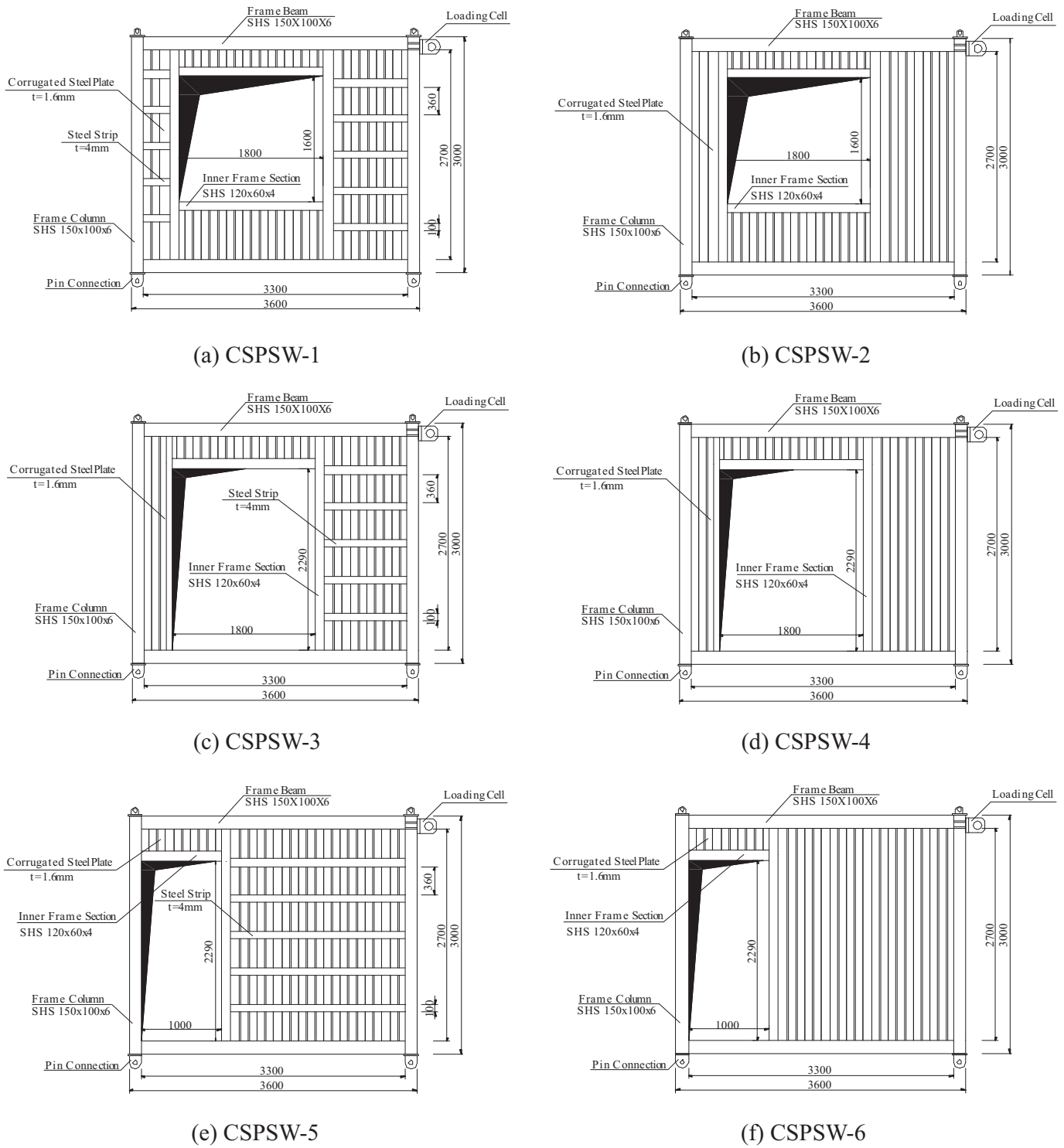

Fig. 2. Shape of corrugations.

Fig. 3. CSPSW Specimen (dimensions in millimeters).

Table 1
Details of CSPSWs specimens.

No.	Openings	Percentage of opening	Width-thickness ratio of the infill plate	Reinforcement
CSPSW-1	Window	0.267	581	Steel Strip
CSPSW-2	Window	0.267	581	–
CSPSW-3	Mid-door	0.381	643	Steel Strip
CSPSW-4	Mid-door	0.381	643	–
CSPSW-5	Side-door	0.212	643	Steel Strip
CSPSW-6	Side-door	0.212	643	–

was not recorded. After the pre-loading program, the normal loading program followed. To ensure the safety of the test program and quality of the test results, the normal loading program was controlled by lateral displacement. Based on ATC-24 [14] and ANSI/AISC 341–10 [15], two cycles of load were applied at each loading step before lateral displacement Δ reached the yield displacement Δ_y. When the specimen yielded, three cycles of load were applied at $1.0\Delta_y$, $1.5\Delta_y$ and $2.0\Delta_y$ loading step. After that, two cycles of load were applied at each loading step. The normal loading program was shown in Fig. 5. The loading program would be ceased immediately as one of these ending conditions happened:

Table 2
Material properties of steel.

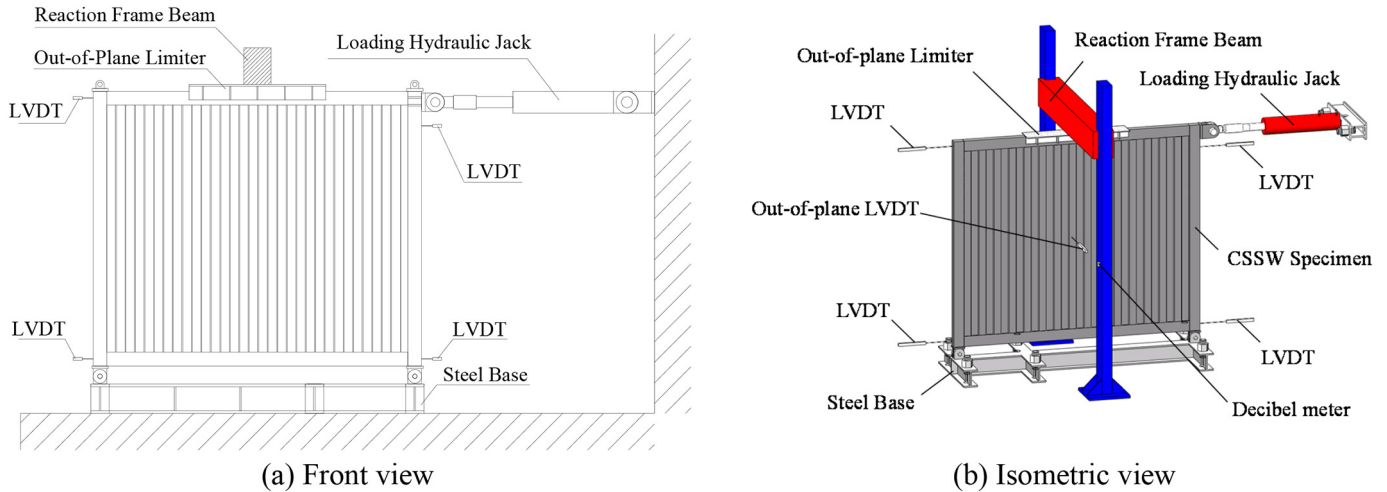| Parts	Thickness (mm)	Elastic modulus (N/mm²)	Yield Strength (N/mm²)	Ultimate Strength (N/mm²)	Ultimate Strain	Elongation (%)
Corrugated steel plates	1.6	195.1	387.8	510.8	0.147	38.5
Steel strip	4.0	200.8	300.8	431.7	0.153	34.1
Inner frame section	4.0	192.1	441.3	543.7	0.170	30.6
Frame beam and column	6.0	194.9	393.8	503.5	0.192	33.8

(a) Front view

(b) Isometric view

Fig. 4. Test setup.

(1)the lateral displacement continued to increase with no increase of load. (2)the load decreased to 85% of the ultimate load. (3)fracture of the specimen would endanger safety [16].

During the loading program, lateral displacement, load, stain and the volume of buckling sound were measured. The load was measured by the dynamic force sensor connected to the loading jack. Five LVDTs measured the lateral displacement at corners of the specimen and the out-of-plane displacement at the center of the specimen. The lateral displacement of the specimen could be defined as difference between the upper and lower displacements. In this way, the effect of the rigid body displacement could be eliminated. Strain on the corrugated steel plate was measured to investigate the tension field. A decibel meter was placed 1.5 m away from the center of the infill plate to measure the volume of the buckling sound during the loading program. The measurement was shown in Fig. 4.
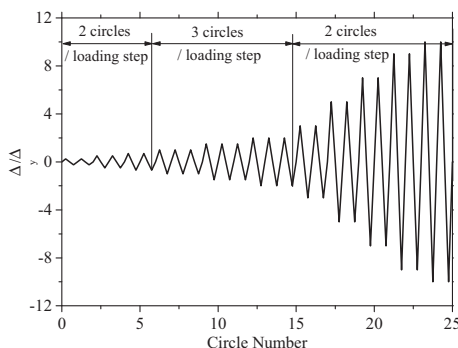

Fig. 5. Loading program.

3. Experimental results and discussion

3.1. General behavior

The load-lateral displacement curves of the specimens were shown in Fig.6. A contrast specimen from reference [17] was added as shown in Fig.6(g). These curves could be divided into four working stages below:

a) At the elastic stage, i.e.,OA period in the curve, the load increased linearly with the lateral displacement. The frames and infill corrugated steel plates of the specimens were in elastic phase. The lateral-load resistance mechanism of the specimens in this stage relied on elastic strength of infill corrugated steel plate. No significant deformations were observed. At the end of this stage, slight elastic buckling of the infill corrugated steel plate was observed during the first circle of the loading step.

b) In the yield stage, i.e.,AB period in the curve, the load increased nonlinearly and hysteretic loops became full. The buckling deformations became obvious in this stage and were usually with loud buckling noise (usually more than 85 dB). The out-of-plane bucking direction changed during the switch of the loading direction with continual buckling noises. Tension fields (Fig. 7(a)) appeared on the infill corrugated steel plate and the angles between the tension fields and lateral direction were about 52° to 72° for different specimens.

Stiffness degradation occurred and platform segments were observed in the load-lateral displacement curves during the loading direction switch of each circle. The platform segments were caused by the global buckling of the infill plate, instead of rigid-body displacement of loading devices. After the global buckling of the infill plate, the lateral-load resistance mechanism relied on the post-buckling
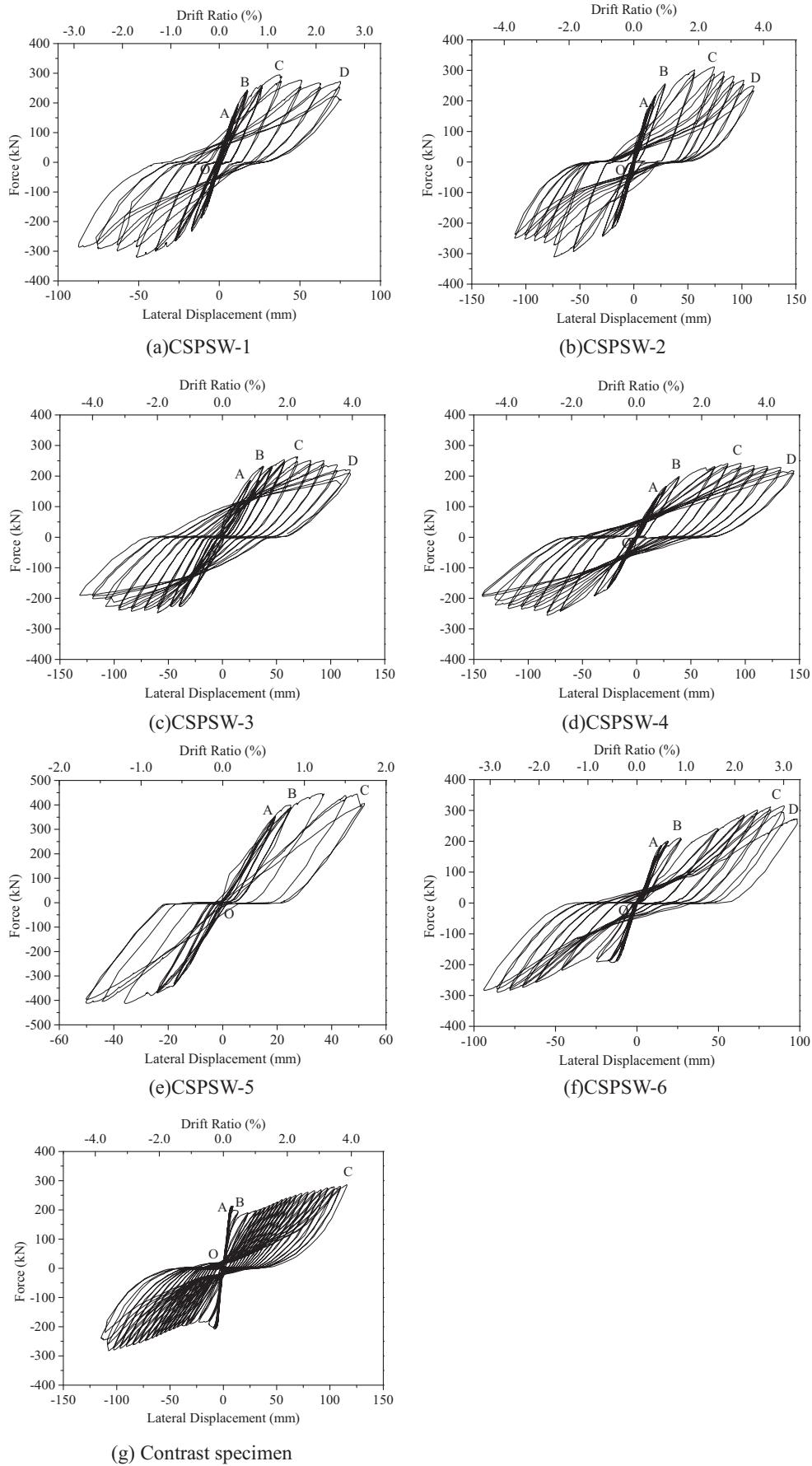
(a)CSPSW-1   (b)CSPSW-2

(c)CSPSW-3   (d)CSPSW-4

(e)CSPSW-5   (f)CSPSW-6

(g) Contrast specimen

Fig. 6. Force-lateral displacement curves of the specimens.

(a) Tension field on infill plate

(b) Fracture of inner frame

(c) Lineal tear on infill plate
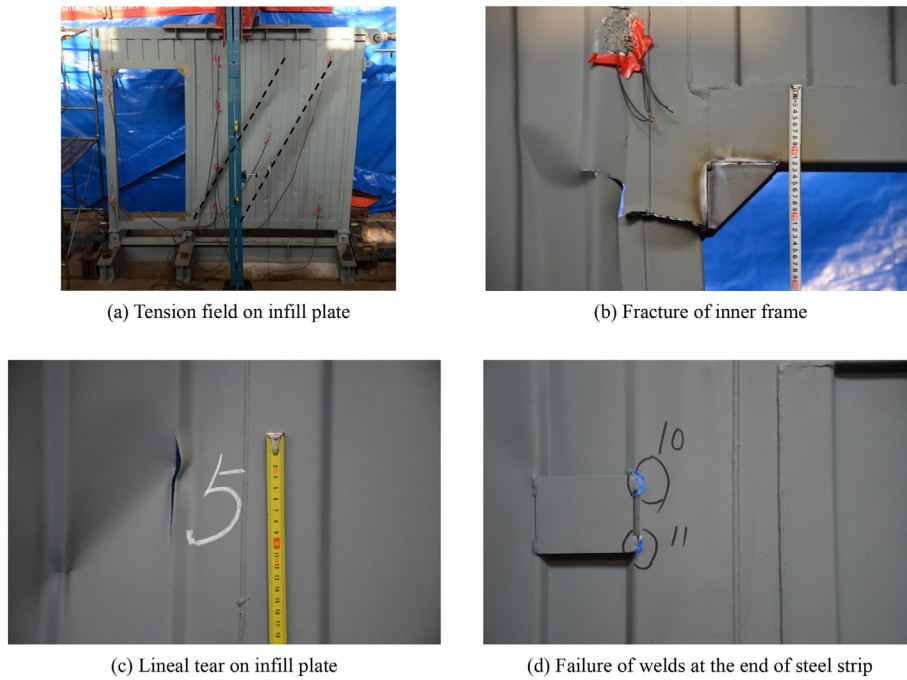
(d) Failure of welds at the end of steel strip

Fig. 7. Observations of CSPSW specimens.

strength of the tension fields. At the end of this stage, residual deformations were observed after unloading of the circle.

c) In the strengthen stage, i.e.,BC period in the curve, the load increased slowly with the lateral displacement due to post-buckling strength of infill corrugated steel plate and reached ultimate point. The hysteretic loops became fuller. The drift ratio reached more than 2.0% and significant lateral deformations of the specimens were observed. The inner frames yielded and came into fracture at all four corners during the stage, as shown in Fig. 7(b). Several tears appeared on the corrugated steel plate and were more severe with the increase of lateral displacement. Most of them were linear except the crossing tear at the center of the specimen, as shown in Fig. 7(c). For the steel strip reinforced specimens, i.e.,CSPSW-1, CSPSW-3, CSPSW-5, the welds at the ends of the steel strips began to fail with sizzle sounds. The fractures of the welds caused tears on the corrugations, as shown in Fig. 7(d). At the end of this stage, the welds between frame beams and columns began to fail.

d) In the ultimate stage, i.e.,CD period in the curve, the loads decreased due to the failure of the welds between frame beams and columns. When the loads were lower than 85% of the ultimate load, the tests were terminated.

The failure mode of all these specimens was the fracture of outer and inner frames. Compared with specimens without steel strips (TS-2, TS-4 and TS-6), the strengthen specimens (TS-1, TS-3 and TS-5) exhibited plastic behavior instead of buckling behavior. At the same drift ratio, the out-of-plane deformations of the infilled plate were smaller on the specimen TS-1, TS-3 and TS-5. The steel strip supported the infilled plate and decreased the out-of-plane deformations.

3.1.1. Specimen CSPSW-1

For specimen CSPSW-1, the elastic stage was from 3.0 mm to 8.4 mm. The force-lateral displacement of the specimen was almost lineal and no significant out-of-plane deformation of the infill corrugated steel plate. Sizzle sounds were heard from the weld of steel strip reinforcements. The yield stage for CSPSW-1 was from 12.0 mm to 18.0 mm. Several welds of the steel strip near the window opening failed with loud noise of 102.3 dB during the loading step (Δ = 12.0 mm). Lineal tears developed along the failure welds during the next loading step. The strengthen

stage was from 24.0 mm to 48.0 mm. The right side of the specimen buckled and tension field appeared on the infill plate at the first cycle of the loading step (Δ = 24.0 mm). The angle between the tension field and lateral direction was about 58°. The inner frame yielded at the loading step (Δ = 36.0 mm) and fractured in full section at the loading step (Δ = 48.0 mm). The position of fracture was at the corners of the window opening. The welds at the ends of the steel strips began to fail with sizzle sounds and teared up the connected corrugated steel plate. The ultimate stage was from 48.0 mm to 84.0 mm. The right side of the specimen buckled and tension field developed with great signification. The infill corrugated steel plate was severely teared. The fracture of the weld between the beams and columns occurred and the test was terminated.

3.1.2. Specimen CSPSW-2

The elastic stage of the specimen CSPSW-2 was from 2.25 mm to 6.3mm. No significant out-of-plane deformation of the infill corrugated steel plate. The yield stage was from loading step 9.0 mm to 18.0 mm. The infill plate buckled and tension field appeared at the load step (Δ= 18.0 mm). The angle between the tension field and lateral direction was about 68°. The strengthen stage was from 27.0 mm to 72.0 mm. The tension field tightened up with a loud sound of 101.5 dB during the second circle of load step (Δ = 45.0 mm). The inner frame yielded at the loading step (Δ = 45.0 mm) and weld of inner frame fractured at the loading step (Δ = 63.0 mm). During the final stage from 72.0 mm to 99.0 mm, inner frame fractured in full section at the corners of the window opening. The weld of the outer frame column and beam at the bottom left corner failed and the test was terminated after the loading step (Δ = 99.0 mm).

3.1.3. Specimen CSPSW-3

The elastic stage of the specimen CSPSW-3 was from 6.0 mm to 18.0mm. No significant out-of-plane deformation of the infill corrugated steel plate. The yield stage was from 24.0 mm to 48.0 mm. The right side of the specimen buckled with a loud noise of 102.2 dB. The angle between the tension field and lateral direction was about 68°. The inner frame column yielded at the top right corner of the mid-door opening during the first circle of the loading step (Δ = 48.0 mm), and fractured at the top left corner during the next circle.

The strengthen stage was from 60.0 mm to 84.0 mm. The inner frame column fractured in full section at the top left corner of the mid-door opening during the second circle of the loading step ($\Delta = 84.0$ mm), causing lineal tears on the left side on the infill plate. The final ultimate stage was from 96.0 mm to 108.0 mm. The inner frame column fractured in full section at the top and bottom left corners of the mid-door opening after the second circle of the loading step ($\Delta = 96.0$ mm). Residual deformations were observed on the frame beam. The weld ofthe outer frame column and beam at the top left corner failed andthe test was terminated during the first attempt of the loading step ($\Delta = 120.0$ mm).

3.1.4. Specimen CSPSW-4

For the specimen CSPSW-4, the elastic stage was from 3.0 mm to 8.4 mm. No significant out-of-plane deformation of the infill corrugated steel plate. The yield stage was from 12.0 mm to 24.0 mm. During this stage, the left side of the specimen buckled with a loud noise of 101.6 dB. The strength stage was from 36.0 mm to 96.0 mm. Tension field appeared on the right side of the specimen during the first circle of the 36 mm-load step. The angle between the tension field and lateral direction was about 65°. The inner frame column yield at all corners of the mid-door opening during this step and fractured after the loading step ($\Delta = 84.0$ mm). Lineal tears appeared on the infill plate. The final ultimate stage was from 96.0 mm to 144.0 mm. The inner frame column fractured in full section at all corners of the mid-door opening during the loading step ($\Delta = 132.0$ mm). Residual deformations were observed on the frame beam after the load was removed. The weld of the outer frame column and beam at the top left corner failed during the loading step ($\Delta = 132.0$ mm). The strength of the specimen at final moment was lower than 85% of the ultimate load and the test was terminated.

3.1.5. Specimen CSPSW-5

The elastic stage was from 3.0 mm to 8.4 mm. No significant out-of-plane deformation of the infill corrugated steel plate. The yield stage was from 12.0 mm to 24.0 mm. The infill corrugated steel plate buckled with a loud noise of 112.8 dB and tension field appeared during the first circle of the loading step ($\Delta = 24.0$ mm). The angle between the tension field and lateral direction was about 59°. The strengthen stage was from 36.0 mm to 48.0 mm. The weld of inner frame column failed at the bottom right corner of the side-door opening during the loading step ($\Delta = 36.0$ mm). The weld of the top steel strip failed during the loading step ($\Delta = 42.0$ mm). The loading program of the specimen CSPSW-5 was terminated in the third stage due to unexpected failure of the welds between frame beams and columns. The reason for the premature failure was the low welding quality of this specimen. As this specimen was firstly tested, all other specimens were double checked and reinforced.

Table 3
Initial stiffness and ultimate strength of the CSPSW specimens.

| No.	Positive direction		Negative direction	
	Initial stiffness (kN/mm)	Ultimate strength (kN)	Initial stiffness (kN/mm)	Ultimate strength (kN)
CSPSW-1	19.8	295.7	21.6	321.6
CSPSW-2	15.3	312.2	15.6	311.8
CSPSW-3	8.9	263.9	8.3	248.4
CSPSW-4	7.9	242.1	7.3	256.3
CSPSW-5	19.2	447.0	22.9	413.5
CSPSW-6	16.5	315.4	20.9	290.8
Contrast specimen	38.8	286.7	39.2	282.6

3.1.6. Specimen CSPSW-6

The elastic stage of the specimen CSPSW-6 was from 2.0 mm to 5.6mm. No significant out-of-plane deformation of the infill corrugated steel plate. The yield stage was from 12.0 mm to 24.0 mm. Infill corrugated steel plate buckled with a noise of 99.2 dB and tension field appeared and tightened up during the loading step ($\Delta = 12.0$ mm). The angle between the tension field and lateral direction was about 56°. The strengthen stage was from 40.0 mm to 80.0 mm. The inner frame column yielded at the top right corner of the side-door opening during the loading step ($\Delta = 56.0$ mm), and fractured at the top right corner during the next circle. Lineal tears appeared around the side-door opening. The final ultimate stage was loading step ($\Delta = 88.0$ mm). The weldof the outer frame column and beam at the top left corner failed and the test was terminated during the first attempt of the loading step ($\Delta = 88.0$ mm). Residual deformations were observed on the left frame column.

3.2. Strength and stiffness

The ultimate strength and stiffness of each corrugated steel plate specimen were revealed as shown in Table3. A specimen in reference [17], with the same dimension and loading program, was added to comparison. This contrast specimen was not a openings worked as a contrast specimen. All specimens in this paper exhibited good ultimate strength. Accidental errors are unavoidable due to complex factors, e.g.,quality of welding, consistency of materials. The maximum error between the ultimate strength of the specimens in positive and negative directions is about 7.9%, which was acceptable for authors.

Fig. 8 compared three groups of force-lateral displacement skeleton curves of the specimens. Each group consisted of two specimens with same openings. One of these was reinforced with steel strips while the

(a) Window opening   (b) Mid-door opening   (c) Side-door opening
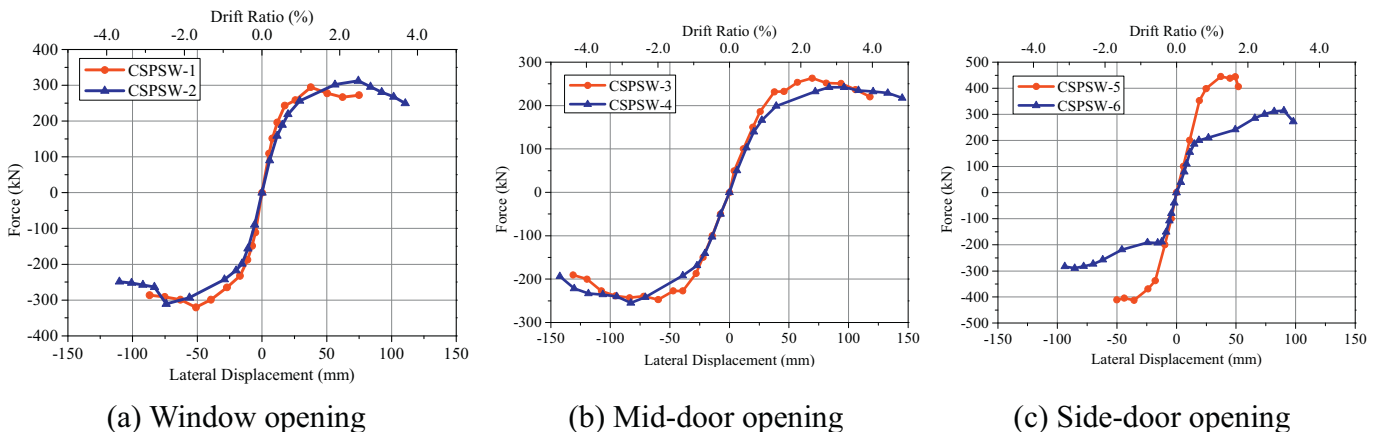
Fig. 8. Skeleton curves of the CSPSW specimens.

(a) Window opening   (b) Mid-door opening   (c) Side-door opening
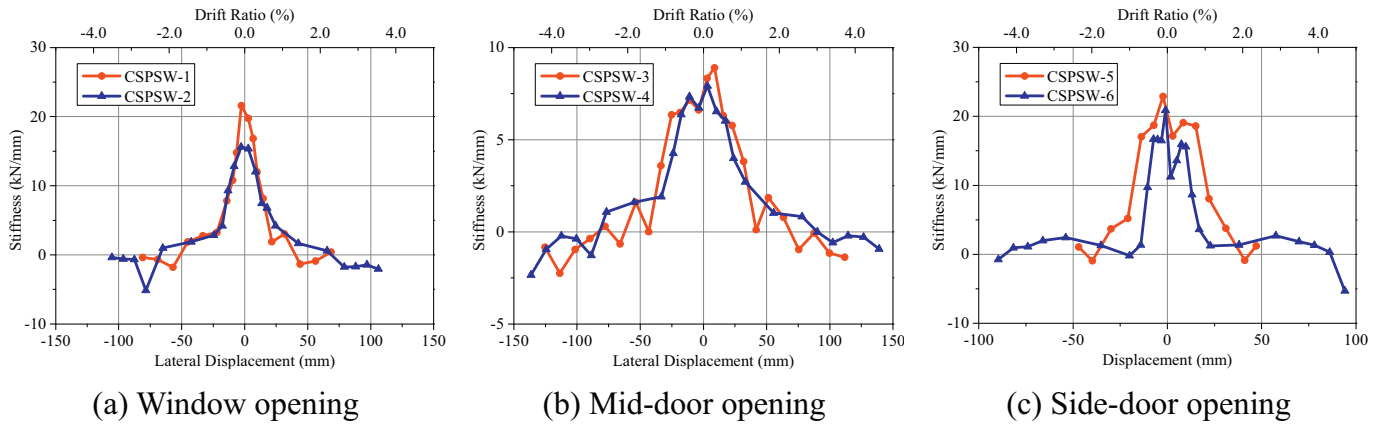
Fig. 9. Stiffness of the CSPSW specimens.

other was not. The shapes of these specimens were similar except for the specimen CSPSW-5 which encountered an unexpected failure due to the low welding quality. The results showed the differences of ultimate strength between the specimens with and without in the three groups were 1.12%, 2.71% and 29.7% respectively. The reason of this observation was that the ultimate strengths of the specimens were determined by the post-buckling strengths of the infill plate. The horizontal steel strips did not have effective restraint on the later formed tension field. It could be concluded conservatively that the differences of the ultimate strengths between the specimens with and without steel strip reinforcement were not significant.

Fig. 9 showed the stiffness of force-lateral displacement skeleton curves of the specimens. The specimens were divided into three groups as above. Stiffness of all specimens was attenuated greatly with increase of lateral displacement. The stiffness of the contrast specimen without openings was significantly higher than that of others. In comparison with ones without steel strip reinforcements, the specimens' stiffness was higher by 25.4%, 11.6% and 11.2% respectively.

The reason of this observation was that the steel strips restricted the out-of-plane displacement of the infill plate. As the out-of–plane stiffness of the CSPSW was strengthened, the buckling of the infilled plate was delayed. Compared with specimens without steel strip reinforcement, strengthened specimens exhibited higher ultimate strength and stiffness. Also the horizontal steel strips connected the columns and acted as batten plates. This indicated that the steel strip reinforcement could improve the initial stiffness of the corrugated steel plate walls, though could not offset the stiffness weakening caused by openings.
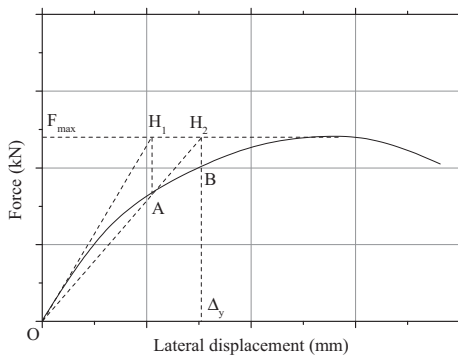
3.3. Ductility and energy dissipation

Ductility and energy dissipation under cyclic load were major parameters for the lateral load resisting systems in buildings structures in seismic hazard area. Generally, all six specimens exhibited good ductility and energy dissipation capacity during the loading program.

The ductility described the load resisting capability after yield and could be evaluated with ductility coefficient, i.e.,the ratio of the yield displacement to the ultimate displacement. For the specimens without obvious yield platforms, yield displacements of all six specimens were found utilizing universal yield moment method in this research [16]. As shown in Fig. 10, the tangent OH_1 from the origin point O intersects the horizontal line of ultimate load at point H_1. The vertical line H_1A intersects the force-lateral displacement curve at the point A. The extension line of OA crosses the horizontal line of ultimate load at point H_2. Another vertical line H_2B is made, crossing the curve at point B. The point B is defined as yield point and the displacement at point B is defined as yield displacement. Table 4 compared the ductility of the specimens. The specimens exhibited good ductility. The ductility coefficients of the specimens (expect for the specimen CSPSW-5 due to low welding quality) were about 2.7–4.3. The results showed that the contrast specimen without openings had the highest ductility coefficient among these specimens (3–4 times of the others'). The ductility coefficients of the specimens with steel strip reinforcements were higher than the ones without the reinforcements by 12.4% (CSPSW-1 vs CSPSW-2) and 8.1% (CSPSW-3 vs CSPSW-4) except CSPSW-5. The unexpected weld fracture caused early failure and significantly decreased the ultimate displacement, causing low ductility coefficient of this specimen. Ignoring this group which could not reflect the true results, it could be concluded that the steel strip reinforcements could improve the ductility of the CSPSWs.

Fig. 10. Universal yield moment method.

Table 4
Ductility of the CSPSW specimens.

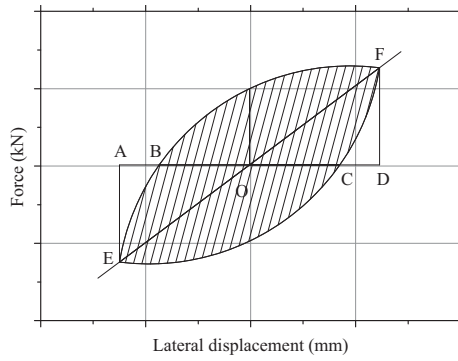| No.	Yield displacement (mm)	Ultimate displacement (mm)	Ultimate story drift ratio	Ductility coefficient
CSPSW-1	19.91	86.80	0.0287	4.36
CSPSW-2	28.97	110.63	0.0367	3.82
CSPSW-3	35.24	131.23	0.0437	3.72
CSPSW-4	42.36	145.10	0.0484	3.42
CSPSW-5	27.05	51.96	0.0173	1.92
CSPSW-6	36.16	98.03	0.0327	2.71
Contrast specimen	7.68	112.02	0.0373	14.59

Fig. 11. Definition of equivalent viscous damping coefficient.

Table 5
Energy dissipation of the specimens.

No	Openings	Maximum energy dissipation (kN·mm)	Maximum equivalent viscous damping coefficients
CSPSW-1	Window opening	16,685	0.145
CSPSW-2	Window opening	17,698	0.117
CSPSW-3	Mid-door opening	30,306	0.202
CSPSW-4	Mid-door opening	29,326	0.159
CSPSW-5	Side-door opening	14,279	0.107
CSPSW-6	Side-door opening	19,570	0.117

Energy dissipation performance describes the capability to absorb seismic energy and is usually evaluated by equivalent viscous damping coefficient. Equivalent viscous damping coefficient h_e is calculated as follows. As shown in Fig. 11, $A_{(BECFB)}$ is the area of shadows, $A_{(OAE+ODF)}$ is the sum area of the tangle OAE and ODF.

$$h_e = \frac{1}{2\pi} \frac{A_{(BECFB)}}{A_{(OAE+ODF)}}$$

Fig. 12 and Fig. 13 respectively illustrated the hysteretic energy dissipation and equivalent viscous damping coefficients. The results showed that the energy dissipation increased with lateral displacement.

When the specimens were at small deformation (drift ratio lower than 1.0%), the differences among these specimens were negligible (less than about 10%). After the yield displacement, the differences became more significant. Compared with the specimens without steel strip reinforcements, the ones with s steel strip reinforcements absorbed more seismic energy during cyclic load and had higher equivalent viscous damping coefficients. Table 5 compared the energy dissipation of three groups of specimens. The differences of equivalent viscous damping coefficients between the specimens with and without steel strip reinforcement was 19.3% (TS-1 vs TS-2), 21.3% (TS-3 vs TS-4) and 9.3% (TS-5 vs
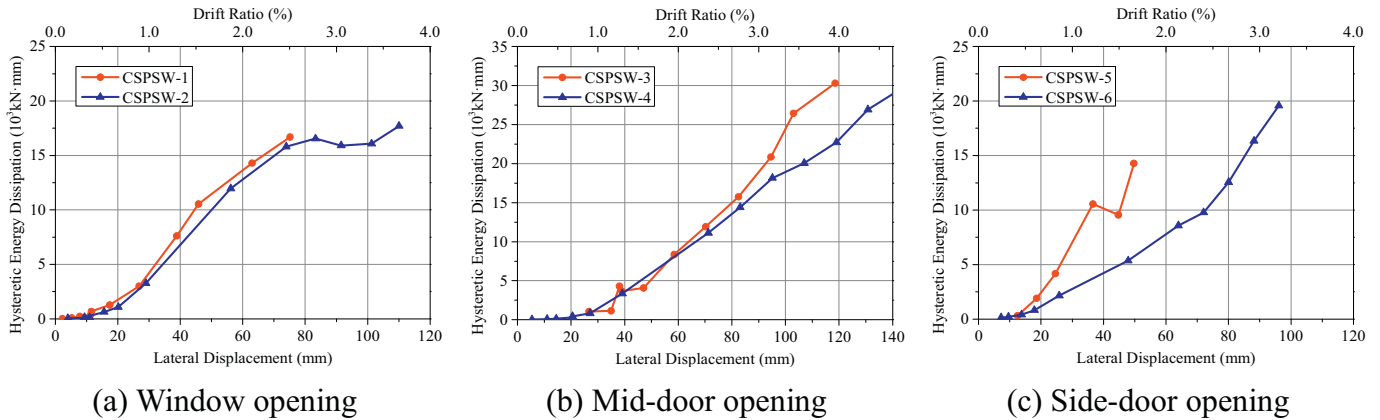

(a) Window opening   (b) Mid-door opening   (c) Side-door opening

Fig. 12. Hysteretic energy dissipation.

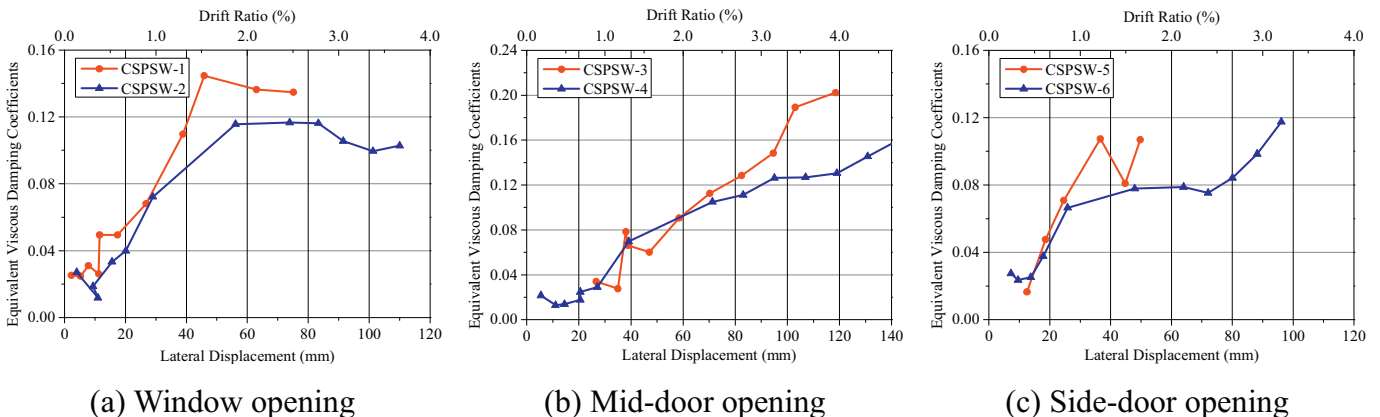(a) Window opening   (b) Mid-door opening   (c) Side-door opening

Fig. 13. Equivalent viscous damping coefficients.

TS-6), respectively. It could be concluded that the steel strip reinforcements could improve energy dissipation performance of the CSPSWs.

The reason of the improvement was that the out-of-plane stiffness was increased due to the steel strips. For the specimens with steel strips, out-of-place buckling was delayed. These specimens exhibited plastic behavior instead of buckling behavior. Plastic deformations occurred on the infilled plate. Compared to buckling deformation, plastic deformations dissipated more during the loading program. That means the higher equivalent viscous damping coefficients compared to the specimens without the steel strips.

4. Conclusion

This paper presented a study of seismic behavior of steel strip reinforced corrugated steel plate walls. An experiment of six full-scale specimens was carried out under quasi-static cyclic loads. These specimens were constrained at two pinned connection to veritably simulate the boundary conditions in modular building structures. The effects of the steel strip reinforcement, including lateral-force resistance mechanism, cyclic performance, stiffness and strength behavior, ductility and energy dissipation capacity, are discussed based on the test results. The following observations and conclusions can be drawn based on the tests results.

1. The observations showed that failure mode of the CSPSWs for the modular building structures was the facture of the weld between the beams and columns. Even reinforced with stiffeners, the failure of the frames still occurred before the infilled plate completely lost the load resisting capacity. The failure of the inner frame around the opening was muck earlier than the failure of the CSPSWs. In practical construction, the failure of the inner frame may cause severe damages to nonstructural components for modular building structures.

2. All the specimens in this paper exhibited favorable seismic performances including stiffness, ultimate strength, ductility and energy dissipation, although the performances of CSPSWs were significantly reduced attributable to the opening compared with the un-opening contrast specimen.

3. The effeteness of steel strip reinforcements was evaluated based on the test results. The steel strip reinforcement had little effect on the ultimate strength, but could improve the performance of stiffness, ductility and energy dissipation. The reason was that steel strips restricted the out-of-plane displacement of the infill corrugated steel plate and delayed the buckling. In this way, the performance of stiffness, ductility and energy dissipation could be improved by the steel strip reinforcements. The ultimate strength was determined by the post-buckling strength of the tension fields, the steel strip. Therefore, the steel strip reinforcement had little effect on the ultimate strength.

References

[1] F. Emami, M. Mofid, A. Vafai, Experimental study on cyclic behavior of trapezoidally corrugated steel shear walls [J], Eng. Struct. 48 (2013) 750–762.
[2] F. Emami, M. Mofid, On the hysteretic behavior of trapezoidally corrugated steel shear walls [J], The Structure Design of Tall and Special Buildings 23 (2012) 2014.
[3] P. Nilsson, M. Al-Emrani, S.R. Atashipour, Transverse shear stiffness of corrugated core steel sandwich panels with dual weld lines [J], Thin-Walled Struct. 117 (2017) 98–112.
[4] C. Dou, Z.Q. Jiang, Y.L. Pi, et al., Elastic shear buckling of sinusoidally corrugated steel plate shear wall [J], Eng. Struct. 121 (2016) 136–146.
[5] J.Z. Tong, Y.L. Guo, Elastic buckling behaviors of steel trapezoidal corrugated shear walls with vertical stiffeners [J], Thin-Walled Struct. 95 (2015) 31–39.
[6] M. Bahrebar, M.Z. Kabir, T. Zirakian, et al., Structural performance assessment of trapezoidally-corrugated and centrally-perforated steel plate shear wall [J], J. Constr. Steel Res. 122 (2016) 584–594.
[7] L.G. Vigh, G.G. Deierlein, E. Miranda, et al., Seismic performance assessment of steel corrugated shear wall system using non-linear analysis [J], J. Constr. Steel Res. 85 (2013) 48–59.
[8] L.G. Vigh, A.B. Liel, G.G. Deierlein, et al., Component model calibration for cyclic behavior of a corrugated shear wall [J], Thin-Walled Struct. 75 (2014) 53–62.
[9] E.B. Machaly, S.S. Safar, M.A. Amer, Numerical investigation on ultimate shear strength of steel plate shear walls [J], Thin-Walled Struct. 84 (2014) 78–90.
[10] E.F. Deng, Y. Ding Zong, et al., Monotonic and cyclic response of bolted connections with welded cover plate for modular steel construction [J], Eng. Struct. 167 (2018) 407–419.
[11] A. Farzampour, J.A. Laman, M. Mofid, Behavior prediction of corrugated steel plate shear walls with openings [J], J. Constr. Steel Res. 114 (2015) 258–268.
[12] GB 50017-2003, Code for design of steel structures [S], 2003, Standards Press of China; Beijing.
[13] GB/T 228.1-2010, Metallic materials-Tensiletesting-Part 1: Method of test at room temperature [S], Standards Press of China, Beijing, 2010.
[14] ATC-24, Guidelines for Cyclic Seismic Testing of Components of Steel Structures [S], Applied Technology Council; Redwood City, 1992.
[15] ANSI/AISC 341-10, Seismic Provisions for Structural Steel Buildings [S], American Institute of Steel Construction, Chicago, 2005.
[16] Z.X. Li, Theory and Technique of Engineering Structure Experiments [M], Press of Tianjin University, Tianjin, 2004.
[17] Y. Ding, E.F. Deng, L. Zong, et al., Cyclic tests on corrugated steel plate shear walls with openings in modularized-constructions [J], J. Constr. Steel Res. 138 (2017) 675–691.